TECHNICAL ARTICLE

Automatic Optical Crack Tracking for Double Cantilever Beam Specimens

B. Krull[1,2], J. Patrick[2,3], K. Hart[2,4], S. White[2,4], and N. Sottos[1,2]

1 Department of Materials Science and Engineering, University of Illinois at Urbana-Champaign, Urbana, IL
2 Beckman Institute for Advanced Science and Technology, University of Illinois at Urbana-Champaign, Urbana, IL
3 Department of Civil and Environmental Engineering, University of Illinois at Urbana-Champaign, Urbana, IL
4 Department of Aerospace Engineering, University of Illinois at Urbana-Champaign, Urbana, IL

Keywords
Fiber-Reinforced Composites, Mode I Fracture, Double Cantilever Beam, Machine Vision

Correspondence
N.R. Sottos,
Department of Materials Science and Engineering,
University of Illinois at Urbana-Champaign,
1304 W. Green St,
Urbana,
IL 61801, USA
Email: n-sottos@illinois.edu

Received: September 19, 2014;
accepted: January 31, 2015

doi:10.1111/ext.12148

Abstract

An automatic crack tracking scheme is developed for measuring the tensile opening (mode I) interlaminar fracture toughness (G_{Ic}) of continuous glass fiber-reinforced composite materials. The technique is directly compared to ASTM standard D5528, which contains a manual procedure to obtain G_{Ic} values from crack length data using a double cantilever beam (DCB) specimen. In this study, a custom computer program with edge detection software rapidly, automatically, and accurately tracks the crack front in translucent DCB specimens by optically monitoring dissimilarities between delaminated and intact portions of the sample. The program combines mechanical testing, image processing, and data collection subroutines into a single interface. The technique is compatible with sample geometries and fabrication processes described in ASTM D5528, and it requires only the addition of a charge-coupled device (CCD) and light source. Compared with the manual techniques outlined in the ASTM standard, the introduced method provides enhanced resolution and reduced workload to determine crack length and resulting G_{Ic} of continuous glass fiber-reinforced composite DCB samples.

Introduction

Interlaminar fracture poses one of the greatest performance concerns for laminated composite materials, limiting reliability and leading to premature catastrophic failure.[1−3] The double cantilever beam (DCB) specimen provides a convenient experimental platform to evaluate resistance to delamination, that is, fracture toughness, for a variety of composite materials and layup sequences.[1−6] A set of comprehensive guidelines for laminated composite DCB sample fabrication, fracture testing, and data analysis are found in ASTM D5528.[6] Although the standard test method is reliable, ASTM D5528 requires manual crack length measurements for each G_{Ic} calculation. As a mid-plane delamination traverses through the DCB, crack length is optically determined from hand-marked delineations along the profile (side) of each sample. Continuous crack length data are not obtained by this method because the delineations are discrete and widely spaced (5 mm). The visual inspection of the ASTM standard is time intensive and potentially subjective.

The need for continuous and automated crack length measurements has driven the development of alternative techniques for improving measurement resolution and accommodating rapid crack propagation rates. Resistance-based methods implement a conductive thin film such as graphite on the side of fracturing DCB samples. A linear decrease in conductance occurs as the crack length increases, which enables electronic monitoring of crack propagation.[7] Time-domain reflectometry (TDR) sensors have also been used to successfully calculate crack length from the reflected pulse time-shift that occurs as a crack front passes between a signal and ground plane.[8] Polymer matrix composites are not typically conductive so electrical traces must be incorporated into the samples for resistance or TDR based techniques. Yoon

et al. attached optical fibers to a DCB specimen and crack length was determined indirectly by using Brillouin scattering to measure the strain distribution.[9] Although less intrusive to sample fabrication, this method was limited to a spatial resolution of 9 mm. Each of these approaches possesses the benefit of providing a more continuous data set than ASTM D5528, but the requirement for specialized sample fabrication is undesirable and any potential alternative should match or surpass the accuracy of the current standard.

Automated optical inspection known as ''machine vision'' has been implemented for a variety of applications including quality control of food, microelectronics, and civil infrastructure.[10–12] Machine vision systems typically use a charge-coupled device (CCD) to record images of a subject. The image then undergoes a post-processing step and subsequent analysis to determine some size, shape, or quality characteristic. The concepts of machine vision have also been applied to crack detection and measurement. Gao et al. applied a gray-level threshold technique to automatically track fatigue crack growth in a compact tension specimen.[13] To address the problem of automatically identifying cracks on complex surfaces, Song et al. used Wigner distribution modeling to analyze images and detect cracks on randomly textured surfaces.[14] However, both techniques require either specialized programming or additional equipment, which limits their broader application. Here, we introduce a method of automatically tracking and measuring cracks in E-glass fiber-reinforced composite DCB specimens. The technique does not require any changes to standard sample preparation. Striving for compatibility with ASTM D5528, our automatic tracking system only requires the addition of a CCD imaging system and light source to the typical test setup. Simple reconfiguration of commercially available software controls both the mechanical testing equipment and image processing for accurate crack length measurements. The software obtains continuous crack length data in real-time with higher spatial resolution than the accepted standard.

Experimental Procedure

DCB sample fabrication

Sixteen plies of an 8-harness satin weave E-glass fabric (Style 7781, Fibre Glast Developments Corp., Brookeville, OH, USA) are stacked in a $[90/0]_8$ layup sequence. An Ethylene tetrafluoroethylene (ETFE) film (25 μm thick) is placed between mid-plies (8/9) serving as a pre-crack. Epoxy resin infiltration (Araldite LY/Aradur 8605, 100:35 by wt., Hunstman Advanced Materials LLC, The Woodlands, TX, USA) is achieved via vacuum-assisted resin transfer molding (VARTM) at 38 Torr (abs) until complete fabric wetting and then decreased to 76 Torr (abs) for 36 h at room temperature (RT) until resin solidification. The fiber-composite panel is post-cured for 2 h at 121°C and 3 h at 177°C. DCB samples are cut using a diamond-blade wet saw from the 4-mm-thick panel to approximately 25 mm wide and 150 mm long (60 mm ETFE, 90 mm neat). Brass hinges (25 mm × 25 mm, McMaster-Carr, Elmhurst, IL, USA) are bonded to outer composite faces on the pre-crack end using a high-strength structural adhesive (Scotch-Weld™ DP 460, 3M™, Maplewood, MN, USA) and allowed to cure for 48 h at RT to ensure sufficient bond-strength before testing. One side (4 mm × 150 mm) of the DCB sample is spray painted matte white (Shock White Acrylic, Montana Gold, Heidelburg, Germany) and allowed to air-dry at RT for 48 h. 5-mm delineations are marked on the painted side beginning 5 mm from the interior pre-crack interface and extending to the free end of the sample.

Fracture test

Each of the DCB specimen cantilever arms is loaded through the bonded hinges in displacement-controlled quasi-static tension to induce mode I fracture propagation along the 0° mid-ply interlaminar region (Fig. 1). The initial pre-crack region (a_0) from the hinge-loading line to the interior ETFE film termination interface is approximately 47 mm. Crosshead speed is (+) 5 mm/min during loading and (−) 25 mm/min for unloading. Overhead and side CCD cameras (A631fc, Basler AG, Ahrensburg, Germany) with mexapixel lenses (LM16HC, Kowa Optimed, Inc., Torrance, CA (USA distributor, manufactured in Japan)) are mounted in the testing area to monitor delamination propagation and record gray-scale images (1024 × 768 pixels, Mono8) every 2 s. This provides an adequate image set to determine crack length at each of the 5-mm delineations for an average crack propagation rate of 5.8 mm/min. Time, load, displacement, and time-stamped image data for crack length correlation are collected using LabVIEW software (v. 2009, National Instruments, Austin, TX, USA).

Crack measurement

For comparison purposes, both manual and automatic crack tracking techniques are implemented for each DCB fracture test. Manual measurements are logged

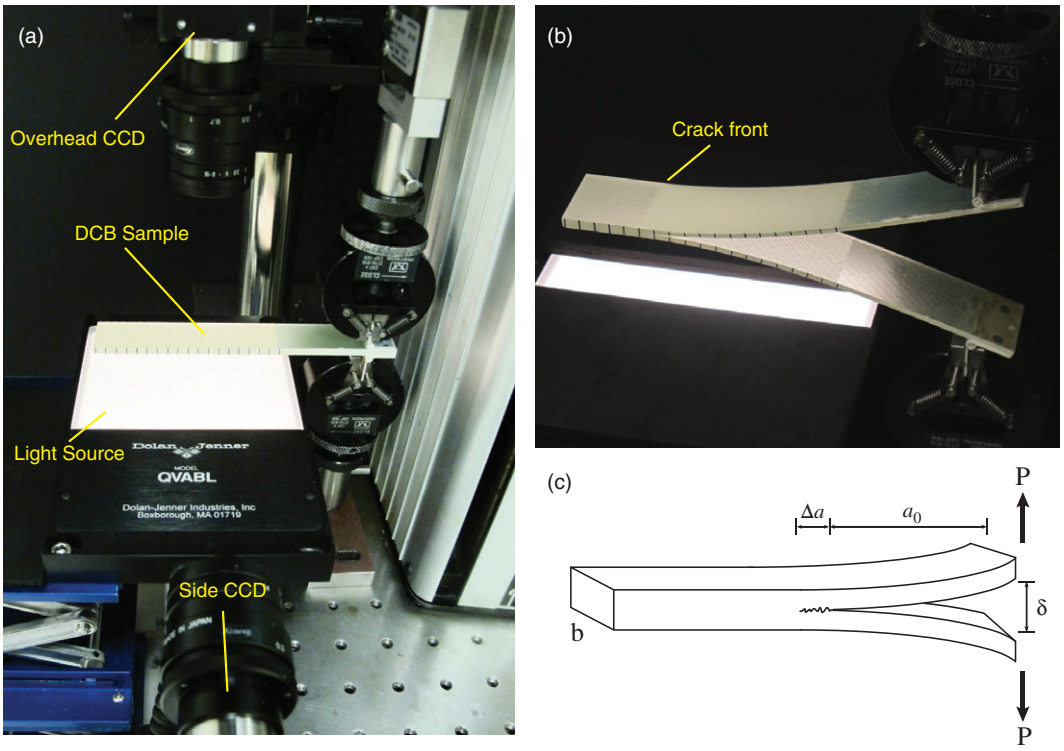

Figure 1 (a) Image of experimental setup showing the light source and overhead with side-mounted CCD cameras. (b) Photograph of DCB sample during the fracture test. (c) Schematic of DCB sample with labeled test variables.

according to the guidelines in ASTM D5528. A time-stamped digital image sequence is acquired during the fracture test by the side-mounted CCD and used to manually determine crack length from the discrete 5-mm crack length delineations along the side of the sample. The timestamp of the image correlates crack position with load and displacement data for subsequent fracture toughness G_{Ic} analysis.

Automatic measurements are acquired by placing a fiber-optic light source (Dolan Jenner: QVABL48 with illuminator DC-950, Dolan Jenner Industries, Boxborough, MA, USA) under the DCB specimen and monitoring crack propagation from an overhead mounted CCD. The translucent E-glass fabric/epoxy matrix composite allows the backlight to provide uniform illumination of the DCB sample. As the fracture test proceeds, delamination between middle plies of the sample causes an apparent contrast between the intact (lighter) portion of the sample and the fractured (darker) portion owing to scattering from the reflective crack plane.[15] The overhead CCD captures images that are fed into the same computer program that controls the mechanical testing equipment. The machine development module in National Instruments LabVIEW software is used to construct a specialized subroutine to continuously monitor and automatically measure the crack length from calibrated optical images (Fig. 2). Crack position is detected based on the intact/fractured contrast differences via machine vision image processing functions. The program searches within a defined region of interest (ROI) to locate the end of the sample and the leading edge of the crack to calculate the crack length,

$$a = a_0 + a_f - a_m \tag{1}$$

where a is the total crack length, a_0 is the pre-crack length, a_f is the available fracture length, and a_m is the optical measurement length (Fig. 3(a)). The software collects image and load–displacement data at a frequency of approximately 10 Hz. The gain of the CCD is programmed to automatically adjust in order to maintain consistent mean gray-level intensity for each image. Without gain adjustment, image brightness may change to an extent that disrupts edge detection.

Optical calibration

An optical calibration factor (OCF) is initially determined as a mm per pixel ratio at the beginning

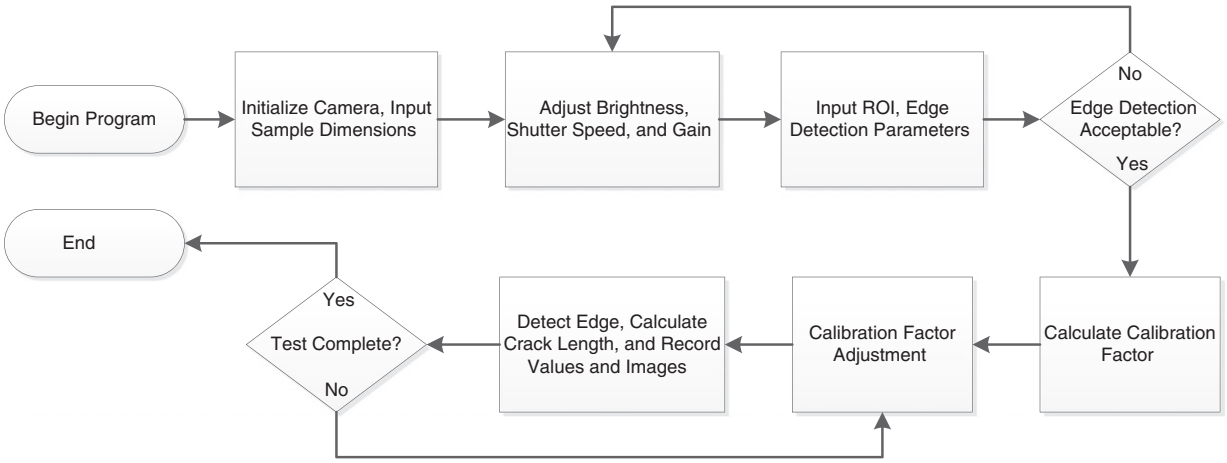

Figure 2 Flowchart of automatic crack tracking and fracture testing computer program.

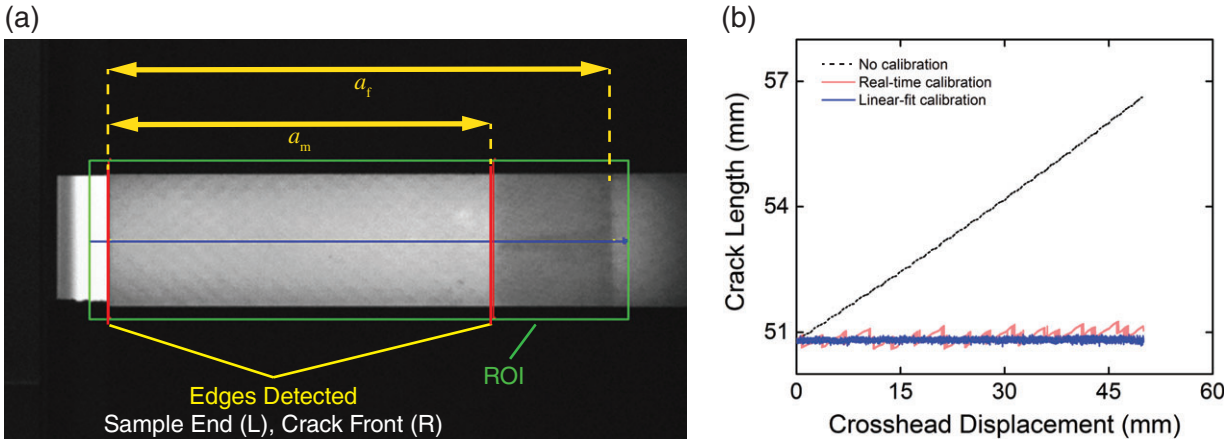

Figure 3 (a) Schematic of edge detection measurement system. The edge detection algorithm sweeps from left to right searching for edges in the region of interest (ROI). The software overlays lines for the ROI (green), edges detected (red), and center of the search region (blue). The pixel distance between the two detected edges (a_m) is used to calculate the crack length from the optical calibration factor (OCF). (b) Crack size as a function of crosshead displacement for the 50.8 mm reference sample. The ''no calibration'' shows an artificial crack length increase as the sample moves closer to the camera. Both calibration adjustment methods (real-time and linear-fit) correct for this artificial increase.

of each test. The software calculates OCF from user-input sample dimensions and the pixel distance (measured via edge detection) between the pre-crack and the end of the DCB specimen (a_f, Fig. 3(a)). The OCF requires *in situ* adjustment during fracture tests as the distance between the overhead CCD and upper surface of the DCB sample decreases as crosshead displacement of the load frame proceeds. As displacement is initiated, samples appear larger and thus, the original OCF becomes invalid. A baseline ''reference'' test is performed using an intact DCB specimen with a 50.8 mm length of black paper attached to the dorsal surface to simulate a constant crack length. The reference is clamped in the top grip only and raised toward the overhead CCD with a total crosshead displacement of 50 mm. As the sample moves closer to the CCD, the detected edge moves pixel-by-pixel and the measured crack length shows an artificial increase of more than 10% (Fig. 3(b)). Owing to this artificial increase, the OCF must be updated throughout the fracture test to ensure accurate crack length measurements.

OCF adjustment is performed by two separate *in situ* methods. A ''real-time calibration'' method adds a second edge detection subroutine to measure the pixel width of the sample. Each new image recalculates the OCF from the real-time pixel width of the sample and the known sample width, which is input by the user before starting the program. A second ''linear-fit calibration'' method is implemented using

the data acquired from the reference sample, which exhibits a nearly linear increase in uncorrected crack length over the displacement range investigated. A least squares linear regression is performed to fit an analytical ''calibration'' curve to the data. The regression analysis for the data reported herein indicates that a decrease of 2.84×10^{-4} mm/pixel in OCF is necessary to maintain proper calibration for each millimeter of crosshead displacement. As long as the camera position and lens focus remain unchanged, this adjustment holds constant for all fracture tests in this investigation. The linear-fit calibration method automatically applies the OCF adjustment during the fracture test based on crosshead displacement readings. Calibration adjustment methods are verified with the reference sample up to a displacement of 50 mm (Fig. 3(b)). Because DCB specimens in actual fracture tests are clamped to both top and bottom test fixtures, the sample mid-plane only moves by one half the crosshead displacement. Therefore, the calibration adjustments are valid up to a total crosshead displacement of 100 mm.

Calibration adjustments

A significant improvement in measurement accuracy occurs with both OCF adjustment methods. Measurements of the 50.8 mm reference sample averaged 50.92 ± 0.34 mm (within 0.7%) for the real-time calibration and 50.81 ± 0.15 mm (within 0.3%) for the linear-fit calibration method. Although both correction methods result in sub-mm accuracy, the error from real-time calibration is double that of the linear-fit calibration. The error approximates 2 pixels for the real-time calibration and 1 pixel for linear-fit calibration. This difference is a result of the real-time calibration method requiring two-edge detection subroutines; one for calibration from specimen width and the other for crack length measurement. The linear-fit calibration method only requires one-edge detection subroutine for the crack length measurement. The error arises due to pixel shifts that occur during the edge detection process, resulting in double the error for the real-time calibration as it uses two edge detection functions.

An increase in camera resolution over the current 1024×768 pixel would decrease the error for each calibration method. The discrepancy between the calibration adjustment methods would also be reduced with increasing resolution. With higher resolution, the mm/pixel calibration factor would be lower and thus the difference between 2-pixel error and 1-pixel error would decrease. Although the real-time calibration is unaffected by small adjustments to test setup, the linear-fit calibration requires camera position and focus to remain constant after determining the OCF adjustment. Thus, an appropriate choice of optics is critical. For a fixed focus lens, verification of adequate depth of field is required over the entire range of sample displacement as edge detection may become less reliable as focus deteriorates. Because all DCB samples in our series of experiments were completely fractured before reaching the 100-mm displacement range (validated by the reference sample), the optics were sufficient for all tests reported herein. The linear-fit calibration method is used for subsequent comparisons to ASTM D5528.

Fracture analysis

Calculations of mode I critical strain energy release rate (G_{Ic}) are performed according to ASTM methodologies.[6] G_{Ic} calculations from discrete (5-mm delineations) and continuous crack length measurements are computed according to the modified beam theory (MBT):

$$G_{Ic} = \frac{3P\delta}{2b\,(a + |\Delta|)} \tag{2}$$

where P is the applied load, δ is the crosshead displacement, b is the specimen width, a is the total crack length and $|\Delta|$ is a correction factor to account for nonzero rotation at the delamination front. This correction factor, $|\Delta|$, is defined as the absolute value of the x-intercept of the line generated from a least squares plot of the cube root of compliance, $C^{1/3} \equiv (\delta/P)^{1/3}$ versus crack length.[4]

Results and Discussion

Crack-tracking comparison

Our dual-camera setup allows direct comparison of the proposed automatic crack tracking method to manual measurements recommended in ASTM D5528. Representative overhead and side images of a DCB sample during testing are shown in Fig. 4. The automatic tracking successfully follows the edge of the crack front as the mid-ply delamination propagates. A representative load–displacement curve is shown in Fig. 5. Owing to an image processing loop speed of approximately 0.1 s, the crack tracking software records the crack position 10 times per second with sub-mm resolution. By comparison, the side-mounted CCD-recorded images for the ASTM D5528 method were acquired at a rate of one image every 2 s. Although faster image recording rates are possible, data management and storage become

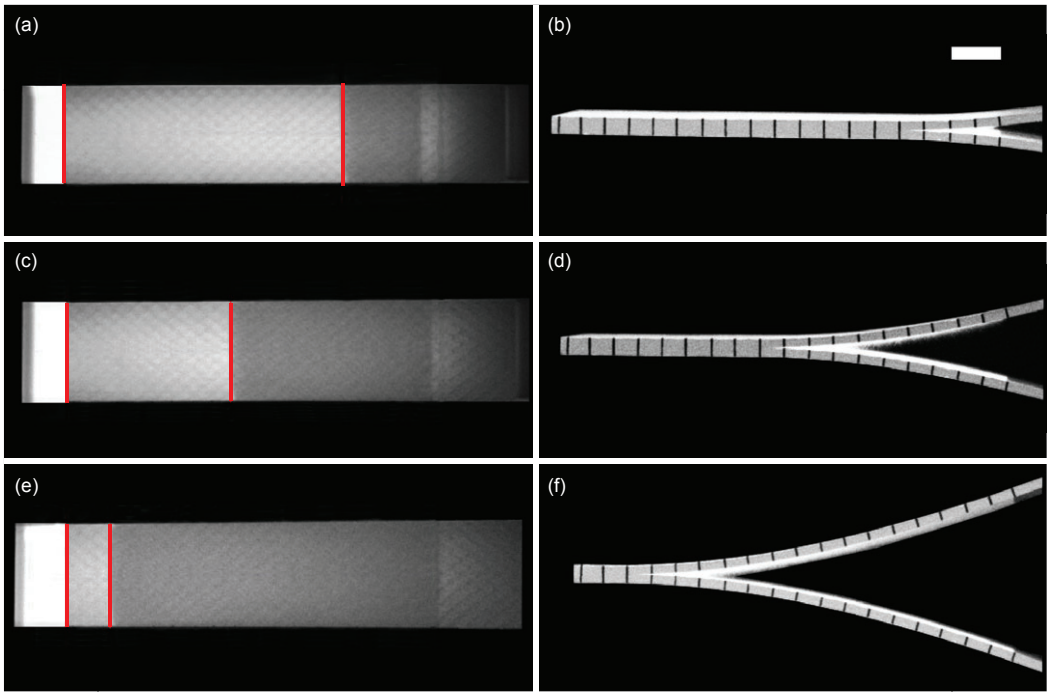

Figure 4 Overhead (a, c, e) and side (b, d, f) images of fracturing DCB specimen at crack lengths 20 mm (a, b); 50 mm (c, d); and 80 mm (e, f). The red lines in overhead images indicate the location of detected edges. The line on the left indicates the end of the sample and the line on the right indicates the location of the crack front (scale bar = 10 mm).

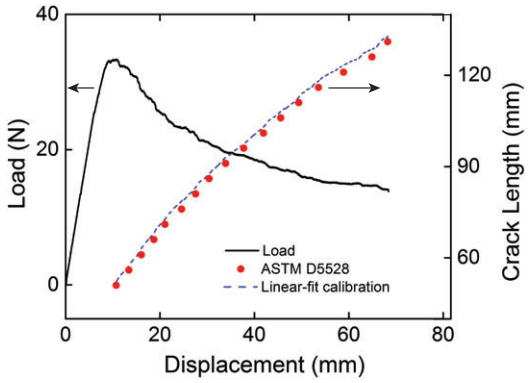

Figure 5 Representative load–displacement behavior of DCB specimens and crack length measurement showing slightly higher values for the automatic tracking technique as compared with the manual ASTM D5528 method.

a concern for long duration tests. The automatic tracking approach removes the need to retain image files as crack length measurements occur on-the-fly.

While the automatic tracking software improves the ease and acquisition rate of crack length measurements, it also records slightly higher crack lengths than those obtained using ASTM D5528 (Fig. 5). Discrepancies of approximately 1.5–2.5 mm are observed over the entire range of crosshead displacement. Sources of error related to the experimental technique(s) were investigated to explain this disparity.

In the ASTM D5528 method, the delineations spaced 5 mm apart are hand drawn onto the side of the sample. Each of the hand-marked delineations approaches 1 mm in width, resulting in a standard accepted ±0.5 mm uncertainty in crack tip position. Hand markings are also difficult to place precisely during sample fabrication.

The experiment operator must next visually determine when the crack has reached the delineation from a series of photographs. The exact position of a crack tip is often difficult to determine, and thus the time at which it reaches each delineation is subjective. However, measurement errors arising from sample preparation and subjective visual analysis have been determined acceptable from round-robin testing reported by ASTM.[2]

Crack front curvature

A more dominant source of error results from the slightly curved shape of the delamination front (Fig. 6(a)). Davidson previously reported anticlastic (transverse) bending of a DCB causes an uneven distribution of critical strain energy release rate (G_{Ic}).

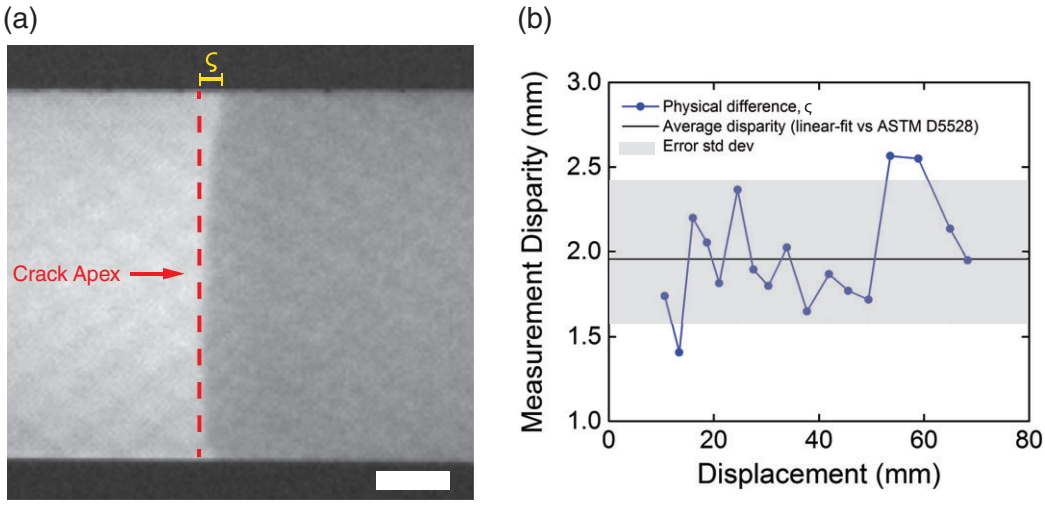

Figure 6 (a) ''Thumbnail'' crack curvature showing the physical difference (ς) in crack length measured from the apex and side of the sample (scale bar = 5 mm). (b) Crack measurement disparity between apex and side detection methods. The average disparity is the difference between ASTM D5528 and the automatic, linear-fit calibration methods for a representative sample.

The uneven distribution is highest in the center of the sample resulting in a ''thumbnail'' crack profile.[5] Crack lengths determined from side observation of the DCB sample will thus be shorter than those recorded by the overhead, automatic edge detection software. Because the software performs an edge detection sweep starting from the free end of the DCB sample, the apex of the crack front is reached first, and recorded as the crack position (Fig. 6(a)).

Figure 6(b) shows the crack length disparity for a representative sample. The crack fronts of overhead images are individually analyzed at each of the discrete (5 mm) crack delineations to determine the physical difference in position between the crack front apex and the crack tip position at the side of the sample. The physical difference between the measurement methods ranges between 1.2 and 2.6 mm greater at the apex of the crack front as compared with the crack length measured from the side of the sample (Fig. 6(b)). For the same sample, an average disparity of 2.0 ± 0.4 mm is observed for linear-fit versus ASTM D5528 methods with no detectable trend with respect to displacement. The average disparity (over all four specimens) in crack length between the ASTM D5528 manual measurements and the linear-fit calibration method is 1.8 ± 0.6 mm. The shape of the crack front appears to be the responsible source of discrepancy between the two methods. Previously reported sample configurations such as alternate pre-crack geometries could be used to straighten the crack front and reduce this effect.[16]

Strain energy release rate

Modified beam theory[4,6] calculations of G_{Ic} are shown for a representative sample in Fig. 7. Manual (ASTM D5528) and automatic (linear-fit calibration) crack measurement methods yield G_{Ic} values of 429 ± 3 and 423 ± 4 J/m^2, respectively, across the entire delamination length. Neither method is consistently higher or lower over the entire range of crack lengths; however, the average G_{Ic} is higher for the ASTM D5528 measurements in all samples owing to lower crack-length measurement values obtained from the side images. Figure 8 shows the average G_{Ic} for all four specimens tested with both manual (ASTM) and automatic (linear-fit calibration) crack tracking methods. Despite averaging nearly 2-mm disparity in crack length, the two methods differ in G_{Ic} by less than 1%. Thus, the automatic crack tracking technique and ASTM D5528 provide comparable data for mode I fracture toughness evaluation of composite DCB specimens.

While discrepancy is marginal in these experiments, the automatic crack tracking method can be considered more conservative than ASTM D5528 because the apex of the crack front yields a larger crack length and reduces the calculated value of G_{Ic}. Measurement differences could be more significant for multidirectional layup sequences that yield greater crack front curvature.[17,18] Future iterations of the crack measuring subroutines could also be adapted to account for crack front curvature by determining a maximum, minimum, or mean delamination length.

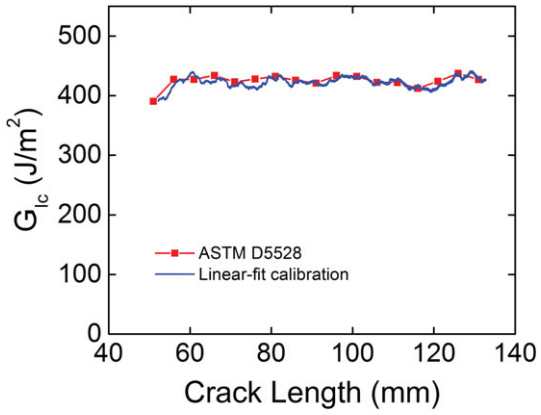

Figure 7 G_{Ic} calculated from modified beam theory (MBT) for manual crack length measurements according to ASTM D5528 and the automatic, linear-fit calibration method for one representative sample.

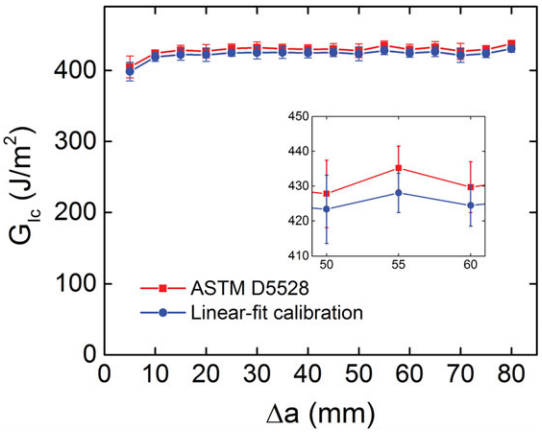

Figure 8 Average G_{Ic} calculated via MBT from manual crack length measurements performed according to ASTM D5528 and the automatic, linear-fit calibration method. (Inset) Magnified data subset showing overlap of error between methods (error bars represent the standard deviation from four samples calculated at each 5-mm crack length interval).

Conclusion

Automatic crack tracking in DCB specimens via edge detection software and an overhead CCD camera is simple, reliable, and accurate. Automatic tracking provides a more continuous crack length data set with superior spatial resolution of 0.15 mm (1 pixel) compared with the accepted standard with 5-mm crack delineation spacing and ±0.5 mm measurement uncertainty. The experimental setup is also highly adaptable and inexpensive to implement as it involves minimal equipment additions and is compatible with traditional composite DCB specimen fabrication.

The introduced experimental technique is currently limited to translucent samples, such as glass fiber-reinforced composites. The correct combination of lighting and sample preparation could allow subsequent versions of the program to achieve automatic crack tracking from the side of the sample. By incorporating techniques previously reported on the subject of crack detection,[11,12] our methodology could be enhanced to detect cracks over a wider range of lighting conditions, test geometries, loading rates, and material constituents. Superior image post-processing of gray-scale differences would make less obvious cracks, for example, those on the side of a DCB sample (Fig. 4), easier to track and thus extend the applicability of this method to opaque samples such as carbon fiber-reinforced composites. Moreover, the customizable nature of LabVIEW and similar software packages provides a pathway to implement on-the-fly fracture toughness calculations that would eliminate the need for post-processing data.

Acknowledgments

This work was financially supported by the Air Force Office of Scientific Research (grant number FA9550-10-1-0255 and Multidisciplinary University Research Initiative, Award No. FA9550-09-1-0686, Synthesis, Characterization and Prognostic Modeling of Functionally Graded Hybrid Composites for Extreme Environments), the Office of Naval Research (grant number 392 Navy Sub TX 2009–03143), and the Army Research Laboratory (grant number W911NF-08-2-0010). We extend our gratitude to Dr. Sharlotte Kramer, former postdoctoral research associate at the Beckman Institute for insightful research discussions concerning optics.

References

1. De Moura, M.F.S.F., Campilho, R.D.S.G., Amaro, A.M., and Reis, P.N.B., ''Interlaminar and Intralaminar Fracture Characterization of Composites Under Mode I Loading,'' *Composite Structures* **92**(1):144–149 (2010).
2. Kim, J., and Sham, M., ''Impact and Delamination Failure of Woven-Fabric Composites,'' *Composites Science and Technology* **60**:745–761 (2000).
3. Senthil, K., Arockiarajan, A., Palaninathan, R., Santhosh, B., and Usha, K., ''Defects in Composite Structures: Its Effects and Prediction Methods - a Comprehensive Review,'' *Composite Structures* **106**:139–149 (2013).
4. Hashemi, S., Kinloch, A., and William, J., ''Corrections Needed in Double-Cantilever Beam

Tests for Assessing the Interlaminar Failure of Fibre-Composites,'' *Journal of Materials Science Letters* **2**:125–129 (1989).
5. Davidson, B.D., ''An Analytical Investigation of Delamination Front Curvature in Double Cantilever Beam Specimens,'' *Journal of Composite Materials* **24**(11):1124–1137 (1990).
6. ASTM International. *ASTM D5528*: *Standard Test Methods for Mode I Interlaminar Fracture Toughness of Unidirectional Fiber-Reinforced Polymer Matrix Composites* (2007).
7. Thesken, J.C., ''A Delamination Gage for Carbon Fiber Composites,'' *Experimental Mechanics* **36**(4):388–398 (1996).
8. Yarlagadda, S., Abuobaid, A., Yoon, M. K., Hager, N., and Domszy, R. ''An Automated Technique for Measuring Crack Propagation during Mode I DCB Testing,'' *2004 SEM X International Congress & Exposition on Experimental & Applied Mechanics* (2004), URL http://www.sem.org/proceedings/ConferencePapers-Paper.cfm?ConfPapersPaperID=24880 [accessed 9 September 2011].
9. Yoon, H.J., Song, K.Y., Kim, J.S., Shin, K.B., and Kim, S.C., ''Crack Propagation Monitoring of DCB Composite Specimens Using Distributed Optical Fiber Sensor,'' *Materials Science Forum* **654–656**:2592–2595 (2010).
10. Jarimopas, B., and Jaisin, N., ''An Experimental Machine Vision System for Sorting Sweet Tamarind,'' *Journal of Food Engineering* **89**(3):291–297 (2008).
11. Sun, T.-H., Tseng, C.-C., and Chen, M.-S., ''Electric Contacts Inspection Using Machine Vision,'' *Image and Vision Computing* **28**(6):890–901 (2010).
12. Kim, B.Y., Member, S., Haas, C.T., and Member, R.G., ''Path Planning For Machine Vision Assisted, Teleoperated Pavement Crack Sealer,'' *Journal of Transportation Engineering* **124**:137–143 (1998).
13. Gao, H.L., Shen, S.S., and Yun, Y., ''Fatigue Crack Length Real Time Measurement Method Based on Camera Automatically Tracking and Positioning,'' *Applied Mechanics and Materials* **130–134**:3111–3118 (2011).
14. Song, K.Y., Petrou, M., and Kittler, J., ''Texture Crack Detection,'' *Machine Vision and Applications* **8**(1):63–75 (1995).
15. Pappada, S., Rametta, R., Largo, A., and Maffezzoli, A., ''Low-Velocity Impact Response in Composite Plates Embedding Shape Memory Alloy Wires,'' *Polymer Composites* **33**(5):655–664 (2012).
16. Robinson, P., and Song, D.Q., ''A Modified DCB Specimen for Mode I Testing of Multidirectional Laminates,'' *Journal of Composite Materials* **26**(11):1554–1577 (1992).
17. De Morais, A., de Moura, M., Gonçalves, J.P., and Camanho, P., ''Analysis of crack propagation in double cantilever beam tests of multidirectional laminates,'' *Mechanics of Materials* **35**(7):641–652 (2003).
18. Sebaey, T.A., Blanco, N., Lopes, C.S., and Costa, J., ''Numerical Investigation to Prevent Crack Jumping in Double Cantilever Beam Tests of Multidirectional Composite Laminates,'' *Composites Science and Technology* **71**(13):1587–1592 (2011).